Adjusted ADM systems and their expected stability properties: constraint propagation analysis in Schwarzschild spacetime

Hisa-aki Shinkai* and Gen Yoneda†
* *Computational Science Division, Institute of Physical & Chemical Research (RIKEN), Hirosawa 2-1, Wako, Saitama, 351-0198 Japan*
† *Department of Mathematical Sciences, Waseda University, Shinjuku, Tokyo, 169-8555, Japan*
(Dated: January 7, 2002 (revised version), gr-qc/0110008)

In order to find a way to have a better formulation for numerical evolution of the Einstein equations, we study the propagation equations of the constraints based on the Arnowitt-Deser-Misner formulation. By adjusting constraint terms in the evolution equations, we try to construct an "asymptotically constrained system" which is expected to be robust against violation of the constraints, and to enable a long-term stable and accurate numerical simulation. We first provide useful expressions for analyzing constraint propagation in a general spacetime, then apply it to Schwarzschild spacetime. We search when and where the negative real or non-zero imaginary eigenvalues of the homogenized constraint propagation matrix appear, and how they depend on the choice of coordinate system and adjustments. Our analysis includes the proposal of Detweiler (1987), which is still the best one according to our conjecture but has a growing mode of error near the horizon. Some examples are snapshots of a maximally sliced Schwarzschild black hole. The predictions here may help the community to make further improvements.

I. INTRODUCTION

Computing the Einstein equations numerically is a necessary direction for general relativity research. This approach, so-called numerical relativity, already gives us much feedback to help understand the nature of strong gravity, such as singularity formations, critical behavior of gravitational collapses, cosmology, and so on. Numerical relativity will definitely be required in unveiling gravitational wave phenomena, highly relativistic astrophysical objects, and might be the only tool to discuss different gravitational theories or models [1].

There are several different approaches to simulate the Einstein equations, among them the most robust is to apply 3+1 (space + time) decomposition of spacetime, which was first formulated by Arnowitt, Deser and Misner (ADM) [2] (we refer to this as the "original ADM" system). A current important issue in the 3+1 approach is to control long-term stability of time integrations in simulating black hole or neutron star binary coalescences. So far, the use of fundamental variables (g_{ij}, K_{ij}), the internal 3-metric and extrinsic curvature, has been the most popular approach [3] (we refer to this as the "standard ADM" system). In recent years, however, many groups report that another re-formulation of the Einstein equations provides more stable and accurate simulations. We try here to understand these efforts through "adjusting" procedures to the evolution equations (that we explain later) using eigenvalue analysis of the constraint propagation equations.

At this moment, there may be three major directions to obtain longer time evolutions. The first is to use a modification of the ADM system that was developed by Shibata and Nakamura [4] (and later remodified by Baumgarte and Shapiro [5]). This is a combination of the introduction of new variables, conformal decompositions, rescaling the conformal factor, and the replacement of terms in the evolution equation using momentum constraints. Although there are many studies to show why this re-formulation is better than the standard ADM, as far as we know, there is no definite conclusion yet. One observation [6] pointed out that to replace terms using momentum constraints appears to change the stability properties.

The second direction is to re-formulate the Einstein equations in a first-order hyperbolic form [7] [33]. This is motivated from the expectation that the symmetric hyperbolic system has well-posed properties in its Cauchy treatment in many systems and also that the boundary treatment can be improved if we know the characteristic speed of the system. We note that, in constructing hyperbolic systems, the essential procedures are to adjust equations using constraints and to introduce new variables, normally the spatially derivatived metric. Several groups report

*Electronic address: shinkai@atlas.riken.go.jp
†Electronic address: yoneda@mn.waseda.ac.jp

that the hyperbolic formulation actually has advantages over the direct use of ADM formulation [9, 10, 11, 12]. However it is also reported that there are no drastic changes in the evolution properties *between* hyperbolic systems (weakly/strongly and symmetric hyperbolicity) by systematic numerical studies by Hern [13] based on Frittelli-Reula formulation [14], and by the authors [15] based on Ashtekar's formulation [16, 17, 18][34]. Therefore we may say that the mathematical notion of "hyperbolicity" is not always applicable for predicting the stability of numerical integration of the Einstein equations (See also §4.4.2 in [1]). It will be useful if we have an alternative procedure to predict stability including the effects of the non-principal parts of the equation, which are neglected in the discussion of hyperbolicity.

The third is to construct a robust system against the violation of the constraints, such that the constraint surface is the attractor. The idea was first proposed as "λ-system" by Brodbeck et al [21] in which they introduce artificial flow to the constraint surface using a new variable based on the symmetric hyperbolic system. This idea was tested and confirmed to work as expected in some test simulations by the authors[22] (based on the formulation developed by [23]). Although it is questionable whether the recovered solution is true evolution or not [24], we think that to enforce the decay of errors in its initial perturbative stage is the key to the next improvements. Actually, by studying the evolution equations of the constraints (hereafter we call them constraint propagation) and by evaluating eigenvalues (amplification factors, AFs) of constraint propagation in its homogenized form, we found that a similar "asymptotically constrained system" can be obtained by simply adjusting constraints to the evolution equations, even for the ADM equations [25].

The purpose of this article is to extend our previous study [25] in more general expressions and also to apply the systems to spacetime which has non trivial curvature, Schwarzschild black hole spacetime. The actual numerical simulations require many ingredients to be considered such as the choice of integration schemes, boundary treatments, grid structures and so on. However, we think that our approach to the stability problem through an *implementation to the equations* is definitely one of the aspects that should be improved.

Adjusting evolution equations is not a new idea. Actually the standard ADM system for numerical relativists [3] is adjusted from the original one [2] using the Hamiltonian constraint (See Frittelli's analysis on constraint propagation between the original and standard ADM formulations [26]). Detweiler [27] proposed a system using adjustments so that the L2 norm of constraints may not blow up (we will study this later in detail). Several numerical relativity groups recently report the advantages of the adjusting procedure with a successful example [10, 11]. We try here to understand the background mathematical features systematically by using AFs of constraint propagation.

We conjecture that we can construct an asymptotically constrained system by evaluating the AFs in advance. Especially, we propose that if the amplification factors are negative or pure-imaginary, then the system becomes more stable. This conjecture is already approved by numerical studies [22] in the Maxwell equations and in the Ashtekar version of the Einstein equations on the Minkowskii background. In this article, we show when and where such a feature is available using the ADM equations for Schwarzschild spacetime. Although the analysis here is restricted to the fixed background, we believe that this study clarifies the properties of adjustments and indicates further possibilities.

In section II, we describe our idea of "adjusted systems" generally, and their application to the ADM formulation. We then explain how we calculate the "amplification factors" in the spherically symmetric spacetime in §III, and show several examples in §IV. The concluding remarks are in §V. Appendix A summarizes the constraint propagation equations of the ADM formulation generally, which may be useful for further studies. Appendix B explains briefly a way to obtain maximally sliced Schwarzschild spacetime that is used to obtain Fig.7.

II. ADJUSTED SYSTEMS

A. Procedure and background – general discussion –

We begin with an overview of the adjusting procedure and the idea of background structure, which were described in our previous work [22, 25].

Suppose we have a set of dynamical variables $u^a(x^i, t)$, and their evolution equations

$$\partial_t u^a = f(u^a, \partial_i u^a, \cdots), \tag{2.1}$$

and the (first class) constraints

$$C^\alpha(u^a, \partial_i u^a, \cdots) \approx 0. \tag{2.2}$$

For monitoring the violation of constraints, we propose to investigate the evolution equation of C^α (constraint propagation),

$$\partial_t C^\alpha = g(C^\alpha, \partial_i C^\alpha, \cdots). \tag{2.3}$$

(We do not mean to integrate (2.3) numerically, but to evaluate them analytically in advance.) Then, there may be two major analyses of (2.3); (a) the hyperbolicity of (2.3) if (2.3) forms a first order form, and (b) the eigenvalue analysis of the whole RHS in (2.3) after certain adequate homogenized procedures.

If the evolution equations form a first-order system, the standard hyperbolic PDE analysis is applicable. The analysis is mainly to identify the level of hyperbolicity and to calculate the characteristic speed of the system, from eigenvalues of the principal matrix. We expect mathematically rigorous well-posed features for strongly hyperbolic or symmetric hyperbolic systems. Also we know the characteristic speeds suggest the satisfactory criteria for stable evolutions; such as when they are real, under the propagation speed of the original variables, u^a, and/or within the causal region of the numerical integration scheme that is applied.

For example, the evolution equations of the standard/original ADM formulation, (2.1) [(2.7) and (2.8)], do not form a first-order system, while their constraint propagation equations, (2.3) [(2.11) and (2.12)], form a first-order system. Therefore, we can apply the classification on the hyperbolicity (weakly, strongly or symmetric) to the constraint propagation equations. However, if one adjusts ADM equations with constraints, then this first-order characters will not be guaranteed. Another problem in the hyperbolic analysis is that it only discusses the principal part of the system, and ignores the rest. If there is a method to characterize the non-principal part, then that will help to clarify our understanding of stability. (This importance was mentioned in [1].)

The second analysis, the eigenvalue analysis of the whole RHS in (2.3), may compensate for the above problems. We propose to homogenize (2.3) by a Fourier transformation, e.g.

$$\begin{aligned} \partial_t \hat{C}^\alpha &= \hat{g}(\hat{C}^\alpha) = M^\alpha{}_\beta \hat{C}^\beta, \\ &\text{where } C(x,t)^\rho = \int \hat{C}(k,t)^\rho \exp(ik\cdot x) d^3k, \end{aligned} \tag{2.4}$$

then to analyze the set of eigenvalues, say Λs, of the coefficient matrix, $M^\alpha{}_\beta$, in (2.4). We call Λs the amplification factors (AFs) of (2.3). As we have proposed and confirmed in [22]:

Conjecture:

(a) If the amplification factors have a *negative real-part* (the constraints are forced to be diminished), then we see more stable evolutions than a system which has positive amplification factors.

(b) If the amplification factors have a *non-zero imaginary-part* (the constraints are propagating away), then we see more stable evolutions than a system which has zero amplification factors.

We found heuristically that the system becomes more stable when more Λs satisfy the above criteria [15, 22] [35]. We remark that this eigenvalue analysis requires the fixing of a particular background spacetime, since the AFs depend on the dynamical variables, u^a.

The above features of the constraint propagation, (2.3), will differ when we modify the original evolution equations. Suppose we add (adjust) the evolution equations using constraints

$$\partial_t u^a = f(u^a, \partial_i u^a, \cdots) + F(C^\alpha, \partial_i C^\alpha, \cdots), \tag{2.5}$$

then (2.3) will also be modified as

$$\partial_t C^\alpha = g(C^\alpha, \partial_i C^\alpha, \cdots) + G(C^\alpha, \partial_i C^\alpha, \cdots). \tag{2.6}$$

Therefore, the problem is how to adjust the evolution equations so that their constraint propagations satisfy the above criteria as much as possible.

B. Standard ADM system and its constraint propagation

We start by analyzing the standard ADM system. By "standard ADM" we mean here the most widely adopted system, due to York [3], with the evolution equations,

$$\partial_t \gamma_{ij} = -2\alpha K_{ij} + \nabla_i \beta_j + \nabla_j \beta_i, \tag{2.7}$$

$$\begin{aligned} \partial_t K_{ij} &= \alpha R^{(3)}_{ij} + \alpha K K_{ij} - 2\alpha K_{ik} K^k{}_j - \nabla_i \nabla_j \alpha \\ &\quad + (\nabla_i \beta^k) K_{kj} + (\nabla_j \beta^k) K_{ki} + \beta^k \nabla_k K_{ij}, \end{aligned} \tag{2.8}$$

and the constraint equations,

$$\mathcal{H} := R^{(3)} + K^2 - K_{ij}K^{ij}, \tag{2.9}$$
$$\mathcal{M}_i := \nabla_j K^j{}_i - \nabla_i K, \tag{2.10}$$

where (γ_{ij}, K_{ij}) are the induced three-metric and the extrinsic curvature, (α, β_i) are the lapse function and the shift covector, ∇_i is the covariant derivative adapted to γ_{ij}, and $R^{(3)}_{ij}$ is the three-Ricci tensor.

The constraint propagation equations, which are the time evolution equations of the Hamiltonian constraint (2.9) and the momentum constraints (2.10), can be written as

$$\begin{aligned}\partial_t \mathcal{H} &= \beta^j(\partial_j \mathcal{H}) + 2\alpha K\mathcal{H} - 2\alpha\gamma^{ij}(\partial_i \mathcal{M}_j) \\ &\quad + \alpha(\partial_l \gamma_{mk})(2\gamma^{ml}\gamma^{kj} - \gamma^{mk}\gamma^{lj})\mathcal{M}_j - 4\gamma^{ij}(\partial_j\alpha)\mathcal{M}_i, \qquad (2.11)\\ \partial_t \mathcal{M}_i &= -(1/2)\alpha(\partial_i \mathcal{H}) - (\partial_i\alpha)\mathcal{H} + \beta^j(\partial_j \mathcal{M}_i) \\ &\quad + \alpha K\mathcal{M}_i - \beta^k\gamma^{jl}(\partial_i\gamma_{lk})\mathcal{M}_j + (\partial_i\beta_k)\gamma^{kj}\mathcal{M}_j. \qquad (2.12)\end{aligned}$$

Further expressions of these constraint propagations are introduced in Appendix A of this article.

C. Adjustment to ADM evolution equations and its effects on constraint propagations

Generally, we can write the adjustment terms to (2.7) and (2.8) using (2.9) and (2.10) by the following combinations (using up to the first derivatives of constraints for simplicity in order to include Detweiler's case, see the next subsection),

$$\text{adjustment term of } \partial_t\gamma_{ij}: \quad + P_{ij}\mathcal{H} + Q^k{}_{ij}\mathcal{M}_k + p^k{}_{ij}(\nabla_k\mathcal{H}) + q^{kl}{}_{ij}(\nabla_k\mathcal{M}_l), \tag{2.13}$$
$$\text{adjustment term of } \partial_t K_{ij}: \quad + R_{ij}\mathcal{H} + S^k{}_{ij}\mathcal{M}_k + r^k{}_{ij}(\nabla_k\mathcal{H}) + s^{kl}{}_{ij}(\nabla_k\mathcal{M}_l), \tag{2.14}$$

where P, Q, R, S and p, q, r, s are multipliers (please do not confuse R_{ij} with three Ricci curvature that we write as $R^{(3)}_{ij}$).

According to this adjustment, the constraint propagation equations are also modified as

$$\partial_t\mathcal{H} = (2.11) + H_1^{mn}(2.13) + H_2^{imn}\partial_i(2.13) + H_3^{ijmn}\partial_i\partial_j(2.13) + H_4^{mn}(2.14), \tag{2.15}$$
$$\partial_t\mathcal{M}_i = (2.12) + M_{1i}{}^{mn}(2.13) + M_{2i}{}^{jmn}\partial_j(2.13) + M_{3i}{}^{mn}(2.14) + M_{4i}{}^{jmn}\partial_j(2.14). \tag{2.16}$$

with appropriate changes in indices. (See detail in Appendix A. The definitions of $H_1, \cdots, M_1, \cdots$ are also there.)

D. Examples of adjustments

We show several examples of adjustments here.

The first test is to show the differences between the standard ADM [3] and the original ADM system [2]. In terms of (2.13) and (2.14), the adjustment,

$$R_{ij} = \kappa_F\alpha\gamma_{ij}, \tag{2.17}$$

will distinguish two, where κ_F is a constant and set the other multipliers zero. Here $\kappa_F = 0$ corresponds to the standard ADM (no adjustment), and $\kappa_F = -1/4$ to the original ADM (without any adjustment to the canonical formulation by ADM). As one can check the adjusted constraint propagation equations in Appendix A, adding R_{ij} term keeps the constraint propagation in a first-order form. Frittelli [26] (see also [25]) pointed out that the hyperbolicity of constraint propagation equations is better in the standard ADM system.

The second example is the one proposed by Detweiler [27]. He found that with a particular combination (see below), the evolution of the energy norm of the constraints, $\mathcal{H}^2 + \mathcal{M}^2$, can be negative definite when we apply the maximal slicing condition, $K = 0$. His adjustment can be written in our notation in (2.13) and (2.14), as

$$P_{ij} = -\kappa_L\alpha^3\gamma_{ij}, \tag{2.18}$$
$$R_{ij} = \kappa_L\alpha^3(K_{ij} - (1/3)K\gamma_{ij}), \tag{2.19}$$
$$S^k{}_{ij} = \kappa_L\alpha^2[3(\partial_{(i}\alpha)\delta^k_{j)} - (\partial_l\alpha)\gamma_{ij}\gamma^{kl}], \tag{2.20}$$
$$s^{kl}{}_{ij} = \kappa_L\alpha^3[\delta^k_{(i}\delta^l_{j)} - (1/3)\gamma_{ij}\gamma^{kl}], \tag{2.21}$$

everything else is zero, where κ_L is a constant. Detweiler's adjustment, (2.18)-(2.21), does not put constraint propagation equation to a first order form, so we cannot discuss hyperbolicity or the characteristic speed of the constraints. We confirmed numerically, using perturbation on Minkowskii spacetime, that Detweiler's system provides better accuracy than the standard ADM, but only for small positive κ_L. See the Appendix of [25].

There are infinite ways of adjusting equations. Actually one of our criteria, the negative real AFs, requires breaking the time-symmetric features of the standard ADM system (when we apply them to the time-symmetric background metric). One observation by us [25] is that such AFs are available if we adjust the terms which break the time reversal symmetry of the evolution equations. That is, by reversing the time ($\partial_t \to -\partial_t$), there are variables which change their signatures $[K_{ij}, \partial_t\gamma_{ij}, \mathcal{M}_i, \cdots]$, while not $[g_{ij}, \partial_t K_{ij}, \mathcal{H}, \cdots]$. (Here we are assuming the 3-metric γ_{ij} has plus parity for time reversal symmetry). So that the multiplier, for example, P_{ij} in (2.13) is desired to have plus parity in order to break the minus parity of $\partial_t\gamma_{ij}$ equation.

We list several combinations of adjustments in Table I and Table III. (Table I shows the ones we have plotted, and the list of plots is in Table II). We defined the adjustment terms so that their positive multiplier parameter, $\kappa > 0$, makes the system *better* in stability according to our conjecture. (Here *better* means in accordance with our conjecture in §II A). In this article, we do not discuss the ranges of the effective multiplier parameter, κ, since the range depends on the characteristic speeds of the models and numerical integration schemes as we observed in [22].

We show how these adjustments change the AFs in Schwarzschild spacetime in §IV.

III. CONSTRAINT PROPAGATIONS IN SPHERICALLY SYMMETRIC SPACETIME

From here, we restrict our discussion to spherically symmetric spacetime. We introduce the violation of constraints as its perturbation using harmonics. According to our motivation, the actual procedure to analyze the adjustments is to substitute the perturbed metric to the (adjusted) evolution equations first and to evaluate the according perturbative errors in the (adjusted) constraint propagation equations. However, for the simplicity, we apply the perturbation to the pair of constraints directly and analyze the effects of adjustments in its propagation equations. The latter, we think, presents the feature of constraint propagation more clearly for our purposes.

A. The procedure

The discussion becomes clear if we expand the constraint $C_\mu := (\mathcal{H}, \mathcal{M}_i)^T$ using vector harmonics,

$$C_\mu = \sum_{l,m} \left(A^{lm} a_{lm} + B^{lm} b_{lm} + C^{lm} c_{lm} + D^{lm} d_{lm} \right), \tag{3.1}$$

where we choose the basis as

$$a_{lm}(\theta,\varphi) = (Y_{lm}, 0, 0, 0)^T, \tag{3.2}$$
$$b_{lm}(\theta,\varphi) = (0, Y_{lm}, 0, 0)^T, \tag{3.3}$$
$$c_{lm}(\theta,\varphi) = \frac{r}{\sqrt{l(l+1)}}(0, 0, \partial_\theta Y_{lm}, \partial_\varphi Y_{lm})^T, \tag{3.4}$$
$$d_{lm}(\theta,\varphi) = \frac{r}{\sqrt{l(l+1)}}(0, 0, -\frac{1}{\sin\theta}\partial_\varphi Y_{lm}, \sin\theta\, \partial_\theta Y_{lm})^T, \tag{3.5}$$

and the coefficients $A^{lm}, \cdots, D^{lm}$ are functions of (t, r). Here Y_{lm} is the spherical harmonic function,

$$Y_{lm}(\theta,\varphi) = (-1)^{(m+|m|)/2} \sqrt{\frac{(2l+1)}{4\pi}\frac{(l-|m|)!}{(l+|m|)!}}\, P_l^m(\cos\theta) e^{im\varphi}. \tag{3.6}$$

The basis (3.2)-(3.5) are normalized so that they satisfy

$$\langle C_\mu, C_\nu \rangle = \int_0^{2\pi} d\varphi \int_0^\pi C_\mu^* C_\rho\, \eta^{\mu\rho} \sin\theta d\theta, \tag{3.7}$$

where $\eta^{\mu\rho}$ is Minkowskii metric and the asterisk denotes the complex conjugate. Therefore

$$A^{lm} = \langle a^{lm}_{(\nu)}, C_\nu \rangle, \quad \partial_t A^{lm} = \langle a^{lm}_{(\nu)}, \partial_t C_\nu \rangle, \quad \text{etc.} \tag{3.8}$$

In order to analyze the radial dependences, we also express these evolution equations using the Fourier expansion on the radial coordinate,

$$A^{lm} = \sum_k \hat{A}^{lm}_{(k)}(t)\, e^{ikr} \quad \text{etc.} \tag{3.9}$$

So that we can obtain the RHS of the evolution equations for $(\hat{A}^{lm}_{(k)}(t), \cdots, \hat{D}^{lm}_{(k)}(t))^T$ in a homogeneous form.

B. Expression for the standard ADM formulation

We write the spherically symmetric spacetime using a metric,

$$\begin{aligned} ds^2 &= -(\alpha(t,r)^2 - \beta_r(t,r)^2/\gamma_{rr})dt^2 + 2\beta_r(t,r)dtdr \\ &\quad +\gamma_{rr}(t,r)dr^2 + \gamma_{\theta\theta}(t,r)(d\theta^2 + \sin^2\theta d\varphi^2), \end{aligned} \tag{3.10}$$

where α and β_r are the lapse function and the shift vector. γ_{rr} and $\gamma_{\theta\theta}$ are also interpreted as 3-metric in 3+1 decomposition, so that the relevant extrinsic curvature, K_{ij}, become $K_{ij} = \mathrm{diag}(K_{rr}, K_{\theta\theta}, K_{\theta\theta}\sin^2\theta)$ and its trace becomes $K = K_{rr}/\gamma_{rr} + 2K_{\theta\theta}/\gamma_{\theta\theta}$.

According to the procedure in the previous section, we obtain the constraint propagation equations for the standard ADM formulation, (2.11) and (2.12), in the following form:

$$\begin{aligned} \partial_t A^{lm}(t,r) &= 2\alpha K A^{lm} + \beta^r(\partial_r A^{lm}) \\ &\quad -2\alpha\gamma^{rr}(\partial_r B^{lm}) + \big(\alpha(\partial_r\gamma_{rr})\gamma^{rr}\gamma^{rr} - 2\alpha(\partial_r\gamma_{\theta\theta})\gamma^{\theta\theta}\gamma^{rr} - 4\gamma^{rr}(\partial_r\alpha)\big)B^{lm} \\ &\quad -2\alpha\gamma^{\theta\theta} r\sqrt{l(l+1)}C^{lm}, \end{aligned} \tag{3.11}$$

$$\begin{aligned} \partial_t B^{lm}(t,r) &= -(1/2)\alpha\partial_r A^{lm} - (\partial_r\alpha)A^{lm} \\ &\quad +(\alpha K - \beta^r\gamma^{rr}(\partial_r\gamma_{rr}) + (\partial_r\beta_r)\gamma^{rr})B^{lm} + \beta^r\partial_r B^{lm}, \end{aligned} \tag{3.12}$$

$$\partial_t C^{lm}(t,r) = -\frac{\alpha\sqrt{l(l+1)}}{2r}A^{lm} + \alpha K C^{lm} + \beta^r(\frac{1}{r}C^{lm} + \partial_r C^{lm}), \tag{3.13}$$

$$\partial_t D^{lm}(t,r) = \alpha K D^{lm} + \beta^r(\frac{1}{r}D^{lm} + \partial_r D^{lm}), \tag{3.14}$$

and then

$$\begin{aligned} \frac{d}{dt}\hat{A}^{lm}_{(k)}(t) &= (2\alpha K + ik\beta^r)\hat{A}^{lm}_{(k)} \\ &\quad +\big(-2ik\alpha\gamma^{rr} + \alpha(\partial_r\gamma_{rr})\gamma^{rr}\gamma^{rr} - 2\alpha(\partial_r\gamma_{\theta\theta})\gamma^{\theta\theta}\gamma^{rr} - 4\gamma^{rr}(\partial_r\alpha)\big)\hat{B}^{lm}_{(k)} \\ &\quad -2\alpha\gamma^{\theta\theta} r\sqrt{l(l+1)}\hat{C}^{lm}_{(k)}, \end{aligned} \tag{3.15}$$

$$\frac{d}{dt}\hat{B}^{lm}_{(k)}(t) = (-(ik/2)\alpha - (\partial_r\alpha))\hat{A}^{lm}_{(k)} + (\alpha K - \beta^r\gamma^{rr}(\partial_r\gamma_{rr}) + (\partial_r\beta_r)\gamma^{rr} + ik\beta^r)\hat{B}^{lm}_{(k)}, \tag{3.16}$$

$$\frac{d}{dt}\hat{C}^{lm}_{(k)}(t) = -\frac{\alpha\sqrt{l(l+1)}}{2r}\hat{A}^{lm}_{(k)} + (\alpha K + \frac{\beta^r}{r} + ik\beta^r)\hat{C}^{lm}_{(k)}, \tag{3.17}$$

$$\frac{d}{dt}\hat{D}^{lm}_{(k)}(t) = (\alpha K + \frac{\beta^r}{r} + ik\beta^r)\hat{D}^{lm}_{(k)}. \tag{3.18}$$

There is no dependence on m. We see that the expressions are equivalent to the case of flat background spacetime [25] when we take $l = 0$ and $r \to \infty$. Therefore our results also show the behavior of the flat background limit in its large r limit.

C. Example: original ADM formulation

We only present here one example, the comparison between the standard and original ADM systems. By substituting (2.17) into (2.15) and (2.16), we obtain

$$\partial_t\mathcal{H} = (2.11) + 4\kappa_1\alpha K\mathcal{H}, \tag{3.19}$$

$$\partial_t\mathcal{M}_i = (2.12) - 2\kappa_1\alpha(\partial_i\mathcal{H}) - 2\kappa_1(\partial_i\alpha)\mathcal{H}. \tag{3.20}$$

In the spherically symmetric spacetime, this adjustment affects (3.11)-(3.14) as follows:

$$\partial_t A^{lm}(t,r) = (3.11) + 4\kappa_1\alpha K A^{lm}, \tag{3.21}$$
$$\partial_t B^{lm}(t,r) = (3.12) - 2\kappa_1\alpha\partial_r A^{lm} - 2\kappa_1(\partial_r\alpha)A^{lm}, \tag{3.22}$$
$$\partial_t C^{lm}(t,r) = (3.13) - \frac{2\kappa_1\alpha\sqrt{l(l+1)}}{r}A^{lm}, \tag{3.23}$$
$$\partial_t D^{lm}(t,r) = (3.14). \tag{3.24}$$

After homogenization, (3.15)-(3.18) become

$$\frac{d}{dt}\begin{pmatrix}\hat{A}^{lm}_{(k)}\\ \hat{B}^{lm}_{(k)}\\ \hat{C}^{lm}_{(k)}\\ \hat{D}^{lm}_{(k)}\end{pmatrix} = \begin{pmatrix}(3.15)\\ (3.16)\\ (3.17)\\ (3.18)\end{pmatrix} + \begin{pmatrix}4\kappa_1\alpha K & 0 & 0 & 0\\ -2\kappa_1\alpha ik - 2\kappa_1(\partial_r\alpha) & 0 & 0 & 0\\ -2\kappa_1\alpha\sqrt{l(l+1)}/r & 0 & 0 & 0\\ 0 & 0 & 0 & 0\end{pmatrix}\begin{pmatrix}\hat{A}^{lm}_{(k)}\\ \hat{B}^{lm}_{(k)}\\ \hat{C}^{lm}_{(k)}\\ \hat{D}^{lm}_{(k)}\end{pmatrix}. \tag{3.25}$$

The eigenvalues (AFs) Λ^i of the RHS matrix of (3.25) can be calculated by fixing the metric components including the gauge. For example, on the standard Schwarzschild metric (4.1), they are

$$\Lambda^i = (0, 0, \sqrt{a}, -\sqrt{a})$$
$$a = -k^2 + \frac{4Mk^2r^2(r-M) + 2M(2r-M) + l(l+1)r(r-2M) + ikr(2r^2-3Mr-2M^2)}{r^4} \tag{3.26}$$

for the choice of $\kappa_1 = 0$ (the standard ADM), while they are

$$\Lambda^i = (0, 0, \sqrt{b}, -\sqrt{b}), \qquad b = \frac{M(2r-M) + irkM(2M-r)}{r^4} \tag{3.27}$$

for the choice of $\kappa_1 = -1/4$ (the original ADM).

D. Our analytic approach

The above example is the simplest one. In the next section, we will show the AFs of the adjusted systems shown in Table I. We found that to write down the analytical expressions of them is not a good idea due to their length. We will therefore plot AFs to see if the real parts become negative, or if the imaginary parts become non-zero or not.

We used the symbolic calculation software, *Mathematica* and *Maple*, and made plots by checking two independent outputs. These scripts are available upon request.

IV. CONSTRAINT PROPAGATIONS IN SCHWARZSCHILD SPACETIME

A. Coordinates

We present our analysis of the constraint propagation equations in Schwarzschild black hole spacetime,

$$ds^2 = -(1 - \frac{2M}{r})dt^2 + \frac{dr^2}{1-2M/r} + r^2 d\Omega^2, \qquad \text{(the standard expression)} \tag{4.1}$$

where M is the mass of a black hole. For numerical relativists, evolving a single black hole is the essential test problem, though it is a trivial at first sight. The standard expression, (4.1), has a coordinate singularity at $r = 2M$, so that we need to move another coordinate for actual numerical time integrations.

One alternative is the isotropic coordinate,

$$ds^2 = -(\frac{1 - M/2r_{iso}}{1 + M/2r_{iso}})^2 dt^2 + (1 + \frac{M}{2r_{iso}})^4[dr^2_{iso} + r^2_{iso}d\Omega^2], \qquad \text{(the isotropic expression)} \tag{4.2}$$

which is given by the coordinate transformation, $r = (1 + M/2r_{iso})^2 r_{iso}$. Here $r_{iso} = M/2$ indicates the minimum throat radius of the Einstein-Rosen bridge. Bernstein, Hobill and Smarr [28] showed a systematic comparison for numerical integration schemes by applying the coordinate transformation, $r_{iso} = Me^{r_{new}}/2$, further to (4.2).

The expression of the ingoing Eddington-Finkelstein (iEF) coordinate has become popular in numerical relativity for treating black hole boundaries as an excision, since iEF penetrates the horizon without a coordinate singularity. The expression is,

$$ds^2 = -(1-\frac{2M}{r})dt_{iEF}^2 + \frac{4M}{r}dt_{iEF}dr + (1+\frac{2M}{r})dr^2 + r^2 d\Omega^2 \qquad \text{(the iEF expression)} \tag{4.3}$$

which is given by $t_{iEF} = t + 2M\log(r-2M)$ and the radial coordinate is common to (4.1). The geometrical interpretation of the iEF coordinate system is that in addition to having a timelike killing vector, the combination of timelike and radial tangent vectors $\vec{\partial}_t - \vec{\partial}_r$ remains null.

Another expression we test is the Painlevé-Gullstrand (PG) coordinates,

$$ds^2 = -\left(1-\frac{2\,M}{r}\right)dt_{PG}^2 + 2\sqrt{\frac{2\,M}{r}}dt_{PG}\,dr + dr^2 + r^2\,d\Omega^2\ , \qquad \text{(the PG expression)} \tag{4.4}$$

which is given by $t_{PG} = t + \sqrt{8Mr} - 2M\log\{(\sqrt{r/2M}+1)/(\sqrt{r/2M}-1)\}$ and the radial coordinate is common to (4.1). The PG coordinate system can be viewed as that anchored to a family of freely moving observers (time-like) starting at infinity with vanishing velocity [29].

The latter two (iEF/PG) are also different from the former (standard/isotropic) two in the point that their extrinsic curvature on the initial slice ($t_{iEF} = t_{PG} = 0$) is not zero. To conclude first, the effects of adjustments are similar both between the former and between the latter.

In Table. II, we list the combinations (adjustments and coordinates) we plotted.

B. in the standard Schwarzschild coordinate

We show first the case of the standard Schwarzschild coordinate, (4.1), since this example provides a basic overview of our analysis. The cases of the isotropic coordinate, (4.2), will be shown to be quite similar.

In Fig.1(a), the amplification factors (AFs, the eigenvalues of homogenized constraint propagation equations) of the standard ADM formulation are plotted. The solid lines and dotted lines with circles are real parts and imaginary parts of AFs, respectively. (The figure style is common throughout the article.) They are four lines each, but as we showed in (3.26), two of them are zero. The plotting range is $2 < r \leq 20$ in Schwarzschild radial coordinate. The AFs at $r = 2$ are $\pm\sqrt{3/8}$ and 0. The existence of this positive real AF near the horizon is a new result which was not seen in the flat background [25]. We show only the cases with $l = 2$ and $k = 1$, because we judged that the plots of $l = 0$ and other ks are qualitatively the same.

The adjustment (2.17) with $\kappa_F = -1/4$ returns the system back to the original ADM. AFs are (3.27) and we plot them in Fig.1(b). We can see that the imaginary parts are apparently different from those of the standard ADM [Fig.1(a)]. This is the same feature as in the case of the flat background [25]. According to our conjecture, the non-zero imaginary values are better than zeros, so we expect that the standard ADM has a better stability than the original ADM system. Negative κ_F makes the asymptotical real values finite. If we change the signature of κ_F, then AFs are as in Fig.1(c). The imaginary parts become larger than $\kappa_F = 0$, that indicates the constraint propagation involves higher frequency modes.

The adjustment proposed by Detweiler, (2.18)-(2.21), makes the feature completely different. Fig.2(a) and (b) are the case of $\kappa_L = 1/4$ and $1/2$ and (c) is of the different signature of κ_L. A great improvement can be seen in both positive κ_L cases where *all* real parts become negative in large r. Moreover all imaginary parts are apart from zero. These are the desired features according to our conjecture. Therefore we expect the Detweiler adjustment has good stability properties *except* near the black hole region. The AF near the horizon *has* a positive real component. This is not contradictory with the Detweiler's original idea. The idea came from suppressing the *total* L2 norm of constraints on the spatial slice, while our plot indicates the existence of a *local* violation mode. The change of signature of κ_L can be understood just by changing the signature of AFs, and this fact can also be seen to the other examples.

We next show that the partial adjustments of Detweiler's are also not so bad. Fig.3 (a), (b) and (c) are the cases of adjustment that are of only (2.18), (2.20) and (2.21), respectively. [The contribution of (2.19) is absent since $K_{ij} = 0$ in the Schwarzschild coordinate.] By comparing them with Fig.1(a) and Fig.2(b), we see the negative real parts in large r are originated by (2.18) and (2.21), while the former two real parts remain zero. Fig.3(d) used only $P_{ij} = -\kappa_L\alpha\gamma_{ij}$ and everything else is zero, which is a minor modification from (2.18). The contribution is similar, and can be said to be *effective*.

C. in isotropic/iEF/PG coordinates

We next compare AFs between different coordinate expressions. The first test is for the standard ADM formulation. Fig.4 shows AFs for (a) the isotropic coordinate (4.2), (b) the iEF coordinate (4.3), and (c) the PG coordinate (4.4). All plots are on the time slice of $t = 0$ in each coordinate expression. [See Fig.1(a) for the standard Schwarzschild coordinate.] We see that Fig.1(a) and Fig.4(a) are quite similar, while Fig.4(b) and (c) are qualitatively different from the former. This is because the latter expressions (iEF/PG) are asymmetric according to time, i.e. they have non-zero extrinsic curvature.

We note that the constraint propagation equations are invariant for spatial coordinate transformation, but AFs are invariant only for linear transformation. This explains the differences between Fig.1(a) and Fig.4(a), although these are not significant.

We notice that while some AFs in iEF/PG remain positive [Fig.4(b) and (c)] in large r region, that their nature changes due to the adjustments. Fig.5 is for the Detweiler-type adjustment, (2.18)-(2.21), for the isotropic/iEF/PG coordinate cases. [See Fig.2(b) for the standard Schwarzschild coordinate.] Interestingly, all plots indicate that all real parts of AFs are negative, and imaginary parts are non-zero (again except near the black hole region). By arranging the multiplier parameter, for the iEF/PG coordinates, there is a chance to get all negative real AFs outside the black hole horizon. For example, for iEF (PG) coordinate all the real-part goes negative outside the black hole horizon if $\kappa_L > 3.1(1.6)$, while large κ_L may introduce another instability problem [22].

Fig.6 shows the adjustment No.4 in Table. I, which was used in the test of PennState group [11]. The main difference from above is that the adjustment here is only for the radial component of the extrinsic curvature, K_{rr}. The numerical experiments in [11] show better stability for positive κ_μ, a fact that can be seen also from Fig.6: positive κ_μ produces negative real AFs. [See Fig.4(b)(c) for the standard ADM case.]

Such kinds of test can be done with other combinations. In Table.III, we listed our results for more examples. The table includes the above results and is intended to extract the contributions of each term in (2.13) and (2.14). The effects of adjustments (of each $\kappa > 0$ case) to AFs are commented upon for each coordinate system and for real/imaginary parts of AFs, respectively. These judgements are made at the $r \sim O(10M)$ region on their $t = 0$ slice. We hope this table will help further numerical improvements for the community.

D. in maximally-sliced evolving Schwarzschild spacetime

So far, our discussion is limited to one 3-hypersurface. Generally speaking, such an initial-value like analysis may not be enough to determine what combination of adjustments, coordinate system, and gauge conditions are suitable for the numerical evolution problem. Here as the first further step, we show our analysis of several snapshots of maximally sliced Schwarzschild spacetime.

The so-called maximal slicing condition, $K = 0$, is one of the most widely used gauge conditions to fix the lapse function, α, during numerical evolution, since it has a feature of singularity avoidance. The condition will turn to an elliptic equation for α. However, in the case of Schwarzschild spacetime, we can express a maximally-sliced hypersurface at an arbitrary time without full numerical time integration. The recipe is given by Estabrook et al [30], and we introduce the procedure briefly in Appendix B.

By specifying a particular time $\bar{t}$, where $\bar{t}$ is supposed to express the time coordinate on a maximally sliced hypersurface (see detail in Appendix B), we get metric components (α, β and γ_{ij}). The procedure requires us to solve ODE, but it is not a result of time integration. We then calculate AFs as the previous ones.

We show several snapshots in Fig.7. We picked up 3-slices of $\bar{t} = 0, 1, 2, \cdots, 5$ for (a) the standard ADM and (b) Detweiler-type adjustment for the Schwarzschild coordinate. These initial data ($\bar{t} = 0$) match those in Fig.1(a) and Fig.2(b), respectively. It is well known that the maximally-sliced hypersurfaces approach (or stop approaching to the singularity) $r_{min} \to (3/2)M$ as $\bar{t} \to \infty$. The snapshots here correspond to $r_{min} = 2.00, 1.90, 1.76, 1.66, 1.60$ and 1.56 in unit M.

The figures show that AFs are changing along their evolution although not drastically, and also that their evolution behavior is dependent upon the choice of adjustments. The evolution makes the AFs' configuration converge, which is expected from the nature of maximal slicing.

V. CONCLUDING REMARKS

Motivated by performing a long-term stable and accurate numerical simulation of the Einstein equation, we proposed to adjust evolution equations by adding constraint terms by analyzing the constraint propagation equations in advance. The idea is to construct an asymptotically constrained evolution system, which is robust against violation

of the constraint. This method works even for the ADM formulation (which is not a hyperbolic system) against flat background spacetime [25], and here we applied the analyses to a curved spacetime, a spherically symmetric black hole spacetime.

Recently, several numerical relativity groups report the effects of adjustments. They are mostly searching for a suitable combination of multipliers through trial and error. We hope our discussion here helps to understand the background mathematics systematically, though it may not be the perfect explanation. The main difference between our analysis and actual numerical studies is that this is a local analysis only on the evolution equations. The actual numerical results are obtained under a certain treatment of the boundary conditions, the choice of numerical integration schemes and grid structures, and also depend on the accuracy of the initial data. We think, however, that our proposal is an alternative to the hyperbolicity classification in that it includes the non-principal part of the evolution equations, and we expect that the discussion here will provide fundamental information on the stable formulation of the Einstein equations to the community. Although we have not shown any numerical confirmations of our conjecture in this article, we remark that the amplification factors explain the constraint violation behaviors quite well in the Maxwell equations and in the Ashtekar version of the Einstein equation on the flat background[22], and also that one of our examples explains a successful case of Kelly et al [11].

We presented a useful expression for analyzing ADM constraint propagation in general in Appendix A, and several analytic predictions of the adjustments for the Schwarzschild spacetime in Table. III. We searched when and where the negative real or non-zero imaginary eigenvalues of the constraint propagation matrix appear, and how they depend on the choice of coordinate system and adjustments. Our analysis includes the proposal of Detweiler (1987), which is still the best one though it has a growing mode of constraint violation near the horizon.

We observed that the effects of adjustments depend on the choice of coordinate, gauge conditions, and also on its time evolution. Therefore our basic assumption of the constancy of the multipliers may be better to be replaced with more general procedures in our future treatment. We have already started to study this issue by applying the recent development of the computational techniques in classical multi-body dynamical systems [32], and hope that we can present some results soon elsewhere.

Acknowledgments

We thank Y. Erigushi, T. Harada, M. Shibata, M. Tiglio for helpful comments. HS is supported by the special postdoctoral researchers program at RIKEN.

APPENDIX A: GENERAL EXPRESSIONS OF ADM CONSTRAINT PROPAGATION EQUATIONS

For the reader's convenience, we express here the constraint propagation equations generally, considering the adjustments to the evolution equations. We repeat the necessary equations again in order for this appendix to be read independently.

1. The standard ADM equations and constraint propagations

We start by analyzing the standard ADM system, that is, with evolution equations

$$\partial_t \gamma_{ij} = -2\alpha K_{ij} + \nabla_i \beta_j + \nabla_j \beta_i, \tag{A1}$$

$$\partial_t K_{ij} = \alpha R^{(3)}_{ij} + \alpha K K_{ij} - 2\alpha K_{ik} K^k{}_j - \nabla_i \nabla_j \alpha + (\nabla_i \beta^k) K_{kj} + (\nabla_j \beta^k) K_{ki} + \beta^k \nabla_k K_{ij}, \tag{A2}$$

and constraint equations

$$\mathcal{H} := R^{(3)} + K^2 - K_{ij} K^{ij}, \tag{A3}$$

$$\mathcal{M}_i := \nabla_j K^j{}_i - \nabla_i K, \tag{A4}$$

where (γ_{ij}, K_{ij}) are the induced three-metric and the extrinsic curvature, (α, β_i) are the lapse function and the shift covector, ∇_i is the covariant derivative adapted to γ_{ij}, and $R^{(3)}_{ij}$ is the three-Ricci tensor.

The constraint propagation equations, which are the time evolution equations of the Hamiltonian constraint (A3) and the momentum constraints (A4).

a. Expression using $\mathcal{H}$ and $\mathcal{M}_i$ The constraint propagation equations can be written as

$$\begin{aligned}
\partial_t \mathcal{H} &= \beta^j(\partial_j\mathcal{H}) + 2\alpha K\mathcal{H} - 2\alpha\gamma^{ij}(\partial_i\mathcal{M}_j) \\
&\quad +\alpha(\partial_l\gamma_{mk})(2\gamma^{ml}\gamma^{kj} - \gamma^{mk}\gamma^{lj})\mathcal{M}_j - 4\gamma^{ij}(\partial_j\alpha)\mathcal{M}_i, \qquad \text{(A5)} \\
\partial_t \mathcal{M}_i &= -(1/2)\alpha(\partial_i\mathcal{H}) - (\partial_i\alpha)\mathcal{H} + \beta^j(\partial_j\mathcal{M}_i) \\
&\quad +\alpha K\mathcal{M}_i - \beta^k\gamma^{jl}(\partial_i\gamma_{lk})\mathcal{M}_j + (\partial_i\beta_k)\gamma^{kj}\mathcal{M}_j. \qquad \text{(A6)}
\end{aligned}$$

This is a suitable form to discuss hyperbolicity of the system. The simplest derivation of (A5) and (A6) is by using the Bianchi identity, which can be seen in Frittelli [26].

A shorter expression is available, e.g.

$$\begin{aligned}
\partial_t \mathcal{H} &= \beta^l\partial_l\mathcal{H} + 2\alpha K\mathcal{H} - 2\alpha\gamma^{-1/2}\partial_l(\sqrt{\gamma}\mathcal{M}^l) - 4(\partial_l\alpha)\mathcal{M}^l \\
&= \beta^l\nabla_l\mathcal{H} + 2\alpha K\mathcal{H} - 2\alpha(\nabla_l\mathcal{M}^l) - 4(\nabla_l\alpha)\mathcal{M}^l, \qquad \text{(A7)} \\
\partial_t \mathcal{M}_i &= -(1/2)\alpha(\partial_i\mathcal{H}) - (\partial_i\alpha)\mathcal{H} + \beta^l\nabla_l\mathcal{M}_i + \alpha K\mathcal{M}_i + (\nabla_i\beta_l)\mathcal{M}^l \\
&= -(1/2)\alpha(\nabla_i\mathcal{H}) - (\nabla_i\alpha)\mathcal{H} + \beta^l\nabla_l\mathcal{M}_i + \alpha K\mathcal{M}_i + (\nabla_i\beta_l)\mathcal{M}^l, \qquad \text{(A8)}
\end{aligned}$$

or by using Lie derivatives along αn^μ,

$$\begin{aligned}
\pounds_{\alpha n^\mu}\mathcal{H} &= 2\alpha K\mathcal{H} - 2\alpha\gamma^{-1/2}\partial_l(\sqrt{\gamma}\mathcal{M}^l) - 4(\partial_l\alpha)\mathcal{M}^l, \qquad \text{(A9)} \\
\pounds_{\alpha n^\mu}\mathcal{M}_i &= -(1/2)\alpha(\partial_i\mathcal{H}) - (\partial_i\alpha)\mathcal{H} + \alpha K\mathcal{M}_i. \qquad \text{(A10)}
\end{aligned}$$

b. Expression using γ_{ij} and K_{ij} In order to check the effects of the adjustments in (A1) and (A2) to constraint propagation, it is useful to re-express (A5) and (A6) using γ_{ij} and K_{ij}. By a straightforward calculation, we obtain an expression as

$$\begin{aligned}
\partial_t \mathcal{H} &= H_1^{mn}(\partial_t\gamma_{mn}) + H_2^{imn}\partial_i(\partial_t\gamma_{mn}) + H_3^{ijmn}\partial_i\partial_j(\partial_t\gamma_{mn}) + H_4^{mn}(\partial_t K_{mn}), \qquad \text{(A11)} \\
\partial_t \mathcal{M}_i &= M_{1i}{}^{mn}(\partial_t\gamma_{mn}) + M_{2i}{}^{jmn}\partial_j(\partial_t\gamma_{mn}) + M_{3i}{}^{mn}(\partial_t K_{mn}) + M_{4i}{}^{jmn}\partial_j(\partial_t K_{mn}), \qquad \text{(A12)}
\end{aligned}$$

where

$$\begin{aligned}
H_1^{mn} &:= -2R^{(3)mn} - \Gamma^p_{kj}\Gamma^k_{pi}\gamma^{mi}\gamma^{nj} + \Gamma^m\Gamma^n \\
&\quad +\gamma^{ij}\gamma^{np}(\partial_i\gamma^{mk})(\partial_j\gamma_{kp}) - \gamma^{mp}\gamma^{ni}(\partial_i\gamma^{kj})(\partial_j\gamma_{kp}) - 2KK^{mn} + 2K^n{}_jK^{mj}, \qquad \text{(A13)} \\
H_2^{imn} &:= -2\gamma^{mi}\Gamma^n - (3/2)\gamma^{ij}(\partial_j\gamma^{mn}) + \gamma^{mj}(\partial_j\gamma^{in}) + \gamma^{mn}\Gamma^i, \qquad \text{(A14)} \\
H_3^{ijmn} &:= -\gamma^{ij}\gamma^{mn} + \gamma^{in}\gamma^{mj}, \qquad \text{(A15)} \\
H_4^{mn} &:= 2(K\gamma^{mn} - K^{mn}), \qquad \text{(A16)} \\
M_{1i}{}^{mn} &:= \gamma^{nj}(\partial_i K^m{}_j) - \gamma^{mj}(\partial_j K^n{}_i) + (1/2)(\partial_j\gamma^{mn})K^j{}_i + \Gamma^n K^m{}_i, \qquad \text{(A17)} \\
M_{2i}{}^{jmn} &:= -\gamma^{mj}K^n{}_i + (1/2)\gamma^{mn}K^j{}_i + (1/2)K^{mn}\delta^j_i, \qquad \text{(A18)} \\
M_{3i}{}^{mn} &:= -\delta^n_i\Gamma^m - (1/2)(\partial_i\gamma^{mn}), \qquad \text{(A19)} \\
M_{4i}{}^{jmn} &:= \gamma^{mj}\delta^n_i - \gamma^{mn}\delta^j_i, \qquad \text{(A20)}
\end{aligned}$$

where we expressed $\Gamma^m = \Gamma^m_{ij}\gamma^{ij}$.

2. Adjustments

Generally, we here write the adjustment terms to (A1) and (A2) using (A3) and (A4) by the following combinations,

$$\begin{aligned}
&\text{adjustment term of} \quad \partial_t\gamma_{ij} : \quad +P_{ij}\mathcal{H} + Q^k{}_{ij}\mathcal{M}_k + p^k{}_{ij}(\nabla_k\mathcal{H}) + q^{kl}{}_{ij}(\nabla_k\mathcal{M}_l), \qquad \text{(A21)} \\
&\text{adjustment term of} \quad \partial_t K_{ij} : \quad +R_{ij}\mathcal{H} + S^k{}_{ij}\mathcal{M}_k + r^k{}_{ij}(\nabla_k\mathcal{H}) + s^{kl}{}_{ij}(\nabla_k\mathcal{M}_l), \qquad \text{(A22)}
\end{aligned}$$

where P, Q, R, S and p, q, r, s are multipliers (please do not confuse R_{ij} with three Ricci curvature that we write as $R^{(3)}_{ij}$). We adjust them only using up to the first derivatives in order to make the discussion simple.

By substituting the above adjustments into (A11) and (A12), we can write the adjusted constraint propagation equations as

$$\begin{aligned}
\partial_t \mathcal{H} &= \text{(original terms)} \\
&+H_1^{mn}[P_{mn}\mathcal{H} + Q^k_{mn}\mathcal{M}_k + p^k{}_{mn}(\nabla_k\mathcal{H}) + q^{kl}{}_{mn}(\nabla_k\mathcal{M}_l)] \\
&+H_2^{imn}\partial_i[P_{mn}\mathcal{H} + Q^k_{mn}\mathcal{M}_k + p^k{}_{mn}(\nabla_k\mathcal{H}) + q^{kl}{}_{mn}(\nabla_k\mathcal{M}_l)] \\
&+H_3^{ijmn}\partial_i\partial_j[P_{mn}\mathcal{H} + Q^k_{mn}\mathcal{M}_k + p^k{}_{mn}(\nabla_k\mathcal{H}) + q^{kl}{}_{mn}(\nabla_k\mathcal{M}_l)] \\
&+H_4^{mn}[R_{mn}\mathcal{H} + S^k_{mn}\mathcal{M}_k + r^k{}_{mn}(\nabla_k\mathcal{H}) + s^{kl}{}_{mn}(\nabla_k\mathcal{M}_l)], \qquad \text{(A23)} \\
\partial_t \mathcal{M}_i &= \text{(original terms)} \\
&+M_{1\,i}{}^{mn}[P_{mn}\mathcal{H} + Q^k_{mn}\mathcal{M}_k + p^k{}_{mn}(\nabla_k\mathcal{H}) + q^{kl}{}_{mn}(\nabla_k\mathcal{M}_l)] \\
&+M_{2\,i}{}^{jmn}\partial_j[P_{mn}\mathcal{H} + Q^k_{mn}\mathcal{M}_k + p^k{}_{mn}(\nabla_k\mathcal{H}) + q^{kl}{}_{mn}(\nabla_k\mathcal{M}_l)] \\
&+M_{3\,i}{}^{mn}[R_{mn}\mathcal{H} + S^k_{mn}\mathcal{M}_k + r^k{}_{mn}(\nabla_k\mathcal{H}) + s^{kl}{}_{mn}(\nabla_k\mathcal{M}_l)] \\
&+M_{4\,i}{}^{jmn}\partial_j[R_{mn}\mathcal{H} + S^k_{mn}\mathcal{M}_k + r^k{}_{mn}(\nabla_k\mathcal{H}) + s^{kl}{}_{mn}(\nabla_k\mathcal{M}_l)]. \qquad \text{(A24)}
\end{aligned}$$

Here the "original terms" can be understood either as (A5) and (A6), or as (A11) and (A12). Therefore, for example, we can see that adjustments to $\partial_t\gamma_{ij}$ do not always keep the constraint propagation equations in the first order form, due to their contribution in the third adjusted term in (A23).

We note that these expressions of constraint propagation equations are equivalent when we include the cosmological constant and/or matter terms.

APPENDIX B: MAXIMALLY SLICING A SCHWARZSCHILD BLACK HOLE

The maximal slicing condition, $K = 0$, is one of the most widely used gauge conditions to fix the lapse function, α, during numerical evolution, since it has a feature of singularity avoidance. The condition will turn into an elliptic equation for α, such as

$$\nabla^i\nabla_i\alpha = (\ {}^{(3)}R + K^2)\alpha = K_{ij}K^{ij}\,\alpha, \qquad \text{(B1)}$$

where we used the Hamiltonian constraint in the second equality. However, for the case of Schwarzschild spacetime, we can express a maximally-sliced hypersurface at an arbitrary time without full numerical integration. The recipe is given by Estabrook et al [30], and we introduce the procedure here briefly.

The goal is to express Schwarzschild geometry with a metric

$$ds^2 = (-\alpha^2 + A^{-1}\beta^2)d\bar{t}^2 + 2\beta d\bar{t}dr + Adr^2 + r^2(d\theta^2 + \sin^2\theta\, d\varphi^2), \qquad \text{(B2)}$$

where $\alpha(\bar{t}, r)$, $\beta(\bar{t}, r)$ and $A(\bar{t}, r)$, and we suppose $\bar{t}$=const. on the maximally-sliced hypersurface.

The original Schwarzschild time coordinate, t, is now the function of $t(\bar{t}, r)$, with

$$\left.\frac{\partial t}{\partial \bar{t}}\right|_{r=const.} = \alpha\sqrt{A} \qquad \text{(B3)}$$

$$\left.\frac{\partial t}{\partial r}\right|_{\bar{t}=const.} = -\frac{\sqrt{A}T}{r^2}\frac{1}{1-2M/r} \qquad \text{(B4)}$$

where T is an arbitrary function of $\bar{t}$, while A is given

$$A = (1 - \frac{2M}{r} + \frac{T^2}{r^4})^{-1}, \qquad \text{(B5)}$$

using both Hamiltonian and momentum constraints. (B4) can be integrated as

$$t = -\frac{T}{M}\int_{M/r}^{X(T)} \frac{1}{1-2x}\frac{1}{\sqrt{1-2x+T^2M^{-4}x^4}}dx, \qquad \text{(B6)}$$

where $X(T)$ is required to be a smaller real root of the quartic equation,

$$1 - 2x + T^2M^{-4}x^4 = 0, \qquad \text{(B7)}$$

in order to be consistent with (B3) under the boundary condition,

$$\text{the smoothness across the Einstein-Rosen bridge, } r = r_{min}, \quad \text{at } t = 0, \tag{B8}$$

that turns $\partial t/\partial r|_{r\to r_{min}} \to \infty$ and $T = T(r_{min}) = \sqrt{r_{min}^3(2M - r_{min})}$.

By identifying $t \sim \bar{t}$ at spatial infinity, we get

$$\bar{t} = -\frac{T}{M}\int_0^{X(T)} \frac{1}{1-2x}\frac{1}{\sqrt{1-2x+T^2M^{-4}x^4}}dx, \tag{B9}$$

where the integration across the pole at $x = 1/2$ is taken in the sense of the principal value.

In summary, if we specified a parameter T ($0 \le T < 3\sqrt{3}/4$ corresponds to $0 \le \bar{t} < \infty$), then we obtain the coordinate time t and $\bar{t}$ from (B6) and (B9) via (B7). Then we obtain the metric components by

$$\alpha(r,T) = \sqrt{1-\frac{2M}{r}+\frac{T^2}{r^4}}\left[1+\frac{dT}{d\bar{t}}\frac{1}{M}\int_0^{M/r}\frac{dx}{(1-2x+T^2M^{-4}x^4)^{2/3}}\right], \tag{B10}$$

$$\beta(r,T) = \alpha A T r^{-2}, \tag{B11}$$

and (B5), where $dT/d\bar{t}$ in (B10) can be calculated using

$$\left(\frac{dT}{d\bar{t}}\right)^{-1} = \frac{d\bar{t}}{dT} = \lim_{Y\to X}\left[\frac{T^2M^{-5}X^4}{(1-2T^2M^{-4}X^3)(2X-1)\sqrt{1-2Y+T^2M^{-4}Y^4}} - \frac{1}{M}\int_0^Y \frac{dx}{(1-2x+T^2M^{-4}x^4)^{3/2}}\right] \tag{B12}$$

They are functions of r and the minimum value of r (that is, at a throat), r_{min}, is given by a larger real root of $r^4 - 2Mr^3 + T^2 = 0$. Note that the fact $r_{min} \to (3/2)M$ when $\bar{t} \to \infty$ indicates the singularity avoidance property of maximal slicing condition. The comparison of this feature with the harmonic slicing condition is seen in [31].

---

[1] For a recent review, see e.g. L. Lehner, Class. Quantum Grav. **18**, R25 (2001).

[2] R. Arnowitt, S. Deser and C. W. Misner,"The Dynamics of General Relativity", in *Gravitation: An Introduction to Current Research*, ed. by L.Witten, (Wiley, New York, 1962).

[3] J. W. York, Jr., "Kinematics and Dynamics of General Relativity", in *Sources of Gravitational Radiation*, ed. by L.Smarr, (Cambridge, 1979) ; L. Smarr, J.W. York,Jr., Phys. Rev. D **17**, 2529 (1978).

[4] T. Nakamura and K. Oohara, in *Frontiers in Numerical Relativity* edited by C.R. Evans, L.S. Finn, and D.W. Hobill (Cambridge Univ. Press, Cambridge, England, 1989). M. Shibata and T. Nakamura, Phys. Rev. D **52**, 5428 (1995).

[5] T. W. Baumgarte and S. L. Shapiro, Phys. Rev. D **59**, 024007 (1999).

[6] M. Alcubierre, G. Allen, B. Brügmann, E. Seidel, and W.M. Suen, Phys. Rev. D **62**, 124011 (2000); M. Alcubierre, B. Brügmann, T. Dramlitsch, J. A. Font, P. Papadopoulos, E. Seidel, N. Stergioulas, and R. Takahashi, Phys. Rev. D **62**, 044034 (2000).

[7] Recent reviews are given by, *e.g.*, O. A. Reula, Livng Rev. Relativ. **1998-3** at `http://www.livingreviews.org/`;
H. Friedrich and A. Rendall, in *Einstein's field equations and their physical interpretation*, ed. by B.G.Schmidt (Springer, Berlin 2000), available as gr-qc/0002074.
See other references in [15], and the most recent study [12].

[8] H-O. Kreiss, O. E. Ortiz, gr-qc/0106085

[9] C. Bona, J. Massó, E. Seidel and J. Stela, Phys. Rev. Lett. **75**, 600 (1995); Phys. Rev. D **56**, 3405 (1997).

[10] M. S. Iriondo and O.A. Reula, gr-qc/0102027.

[11] B. Kelly, P. Laguna, K. Lockitch, J. Pullin, E. Schnetter, D. Shoemaker, and M. Tiglio, Phys. Rev. D **64**, 084013 (2001).

[12] L. E. Kidder, M. A. Scheel and S. A. Teukolsky, Phys. Rev. D **64**, 064017 (2001).

[13] S. D. Hern, PhD thesis, gr-qc/0004036.

[14] S. Frittelli and O. A. Reula, Phys. Rev. Lett. **76**, 4667 (1996). See also J. M. Stewart, Class. Quantum Grav. **15**, 2865 (1998).

[15] H. Shinkai and G. Yoneda, Class. Quantum Grav. **17**, 4799 (2000).

[16] G. Yoneda and H. Shinkai, Phys. Rev. Lett. **82**, 263 (1999).

[17] G. Yoneda and H. Shinkai, Int. J. Mod. Phys. D **9**, 13 (2000).

[18] A. Ashtekar, Phys. Rev. Lett. **57**, 2244 (1986); Phys. Rev. D **36**, 1587 (1987); *Lectures on Non-Perturbative Canonical Gravity* (World Scientific, Singapore, 1991).

[19] G. Calabrese, J. Pullin, O. Sarbach and M. Tiglio, in preparation.
[20] A. Anderson and J. W. York, Jr, Phys. Rev. Lett. **82**, 4384 (1999).
[21] O. Brodbeck, S. Frittelli, P. Hübner and O.A. Reula, J. Math. Phys. **40**, 909 (1999).
[22] G. Yoneda and H. Shinkai, Class. Quantum Grav. **18**, 441 (2001).
[23] H. Shinkai and G. Yoneda, Phys. Rev. D **60**, 101502 (1999).
[24] F. Siebel and P. Hübner, Phys. Rev. D **64**, 024021 (2001).
[25] G. Yoneda and H. Shinkai, Phys. Rev. D **63**, 120419 (2001).
[26] S. Frittelli, Phys. Rev. D **55**, 5992 (1997).
[27] S. Detweiler, Phys. Rev. D **35**, 1095 (1987).
[28] D. Bernstein, D. W. Hobill, and L. L. Smarr, in *Frontiers in Numerical Relativity*, edited by C.R. Evans, L.S. Finn, and D.W. Hobill (Cambridge Univ. Press, 1989)
[29] K. Martel and E. Poisson, gr-qc/0001069 (2000).
[30] F. Estabrook, H. Wahlquist, S. Christensen, B. DeWitt, L. Smarr, and E. Tsiang, Phys. Rev. D. **7**, 2814 (1973).
[31] A. Geyer and H. Herold , Phys. Rev. D. **52**, 6182 (1995), Gen. Rel. Grav. **29**, 1257 (1997).
[32] H. Shinkai, G. Yoneda, and T. Ebisuzaki, in preparation.
[33] We note that rich mathematical theories on PDEs are obtained in a first-order form, while there is a study on linearized ADM equations in a second-order form [8].
[34] [19] reports that there is an apparent difference on numerical stability between these hyperbolicity levels, based on Kidder-Scheel-Teukolsky's reformulation [12] of Anderson-York [20] and Frittelli-Reula [14] formulations.
[35] We note that the *non-zero* eigenvalue feature was conjectured in Alcubierre *et. al.* [6] in order to show the advantage of the conformally-scaled ADM system, but the discussion there is of linearized dynamical equations and not of constraint propagation equations.

No.	name	adjustments (non-zero part)	TRS	1st?	motivations
0	standard ADM	no adjustments	–	yes	
1	original ADM	$R_{ij} = \kappa_F \alpha \gamma_{ij}$	yes	yes	$\kappa_F = -1/4$ makes original ADM
2-a	Detweiler	(2.18)-(2.21), κ_L	no	no	proposed by Detweiler [27]
2-P	Detweiler P-part	$P_{ij} = -\kappa_L \alpha^3 \gamma_{ij}$	no	no	only use P_{ij} term of Detweiler-type
2-S	Detweiler S-part	$S^k{}_{ij} = \kappa_L \alpha^2 [3(\partial_{(i}\alpha)\delta^k_{j)} - (\partial_l \alpha)\gamma_{ij}\gamma^{kl}]$	no	yes	only use $S^k{}_{ij}$ term of Detweiler-type
2-s	Detweiler s-part	$s^{kl}{}_{ij} = \kappa_L \alpha^3 [\delta^k_{(i}\delta^l_{j)} - (1/3)\gamma_{ij}\gamma^{kl}]$	no	no	only use $s^{kl}{}_{ij}$ term of Detweiler-type
3	simplified Detweiler	$P_{ij} = -\kappa_L \alpha \gamma_{ij}$	no	no	similar to above No.2-P, but α monotonic
4	constant R_{rr}	$R_{rr} = -\kappa_\mu \alpha$	no	yes	used by Penn State group [11]

TABLE I: List of adjustments we tested and plotted. (See more cases in Table.III). The column of adjustments are nonzero multipliers in terms of (2.13) and (2.14). The column 'TRS' indicates whether each adjusting term satisfies the time reversal symmetry or not based on the standard Schwarzschild coordinate. ('No' is the candidate that makes asymmetric amplification factors (AFs).) The column '1st?' indicates whether each adjusting term breaks the first-order feature of the standard constraint propagation equation, (2.11) and (2.12). ('Yes' keeps the system first-order, 'No' is the candidate of breaking hyperbolicity of constraint propagation.)

adjustment \ coordinate		standard (4.1)		isotropic (4.2)	iEF (4.3)	PG (4.4)
		exact	maximal	exact	$t_{iEF} = 0$	$t_{PG} = 0$
0	standard ADM	Fig.1(a)	Fig.7(a)	Fig.4(a)	Fig.4(b)	Fig.4(c)
1	original ADM	Fig.1(b)				
2-a	Detweiler	Fig.2	Fig.7(b)	Fig.5(a)	Fig.5(b)	Fig.5(c)
2-P	Detweiler P-part	Fig.3(a)				
2-S	Detweiler S-part	Fig.3(b)				
2-s	Detweiler s-part	Fig.3(c)				
3	simplified Detweiler	Fig.3(d)				
4	constant R_{rr}				Fig.6(a)	Fig.6(b)

TABLE II: List of figures presented in this article. The adjustments are explained in Table. I.

No.	No. in Table.I	adjustment	1st?	TRS	Sch/iso coords. real.	Sch/iso coords. imag.	iEF/PG coords. real.	iEF/PG coords. imag.
0	0	– no adjustments	yes	–	–	–	–	–
P-1	2-P	P_{ij} $-\kappa_L\alpha^3\gamma_{ij}$	no	no	makes 2 Neg.	not apparent	makes 2 Neg.	not apparent
P-2	3	P_{ij} $-\kappa_L\alpha\gamma_{ij}$	no	no	makes 2 Neg.	not apparent	makes 2 Neg.	not apparent
P-3	-	P_{ij} $P_{rr}=-\kappa$ or $P_{rr}=-\kappa\alpha$	no	no	slightly enl.Neg.	not apparent	slightly enl.Neg.	not apparent
P-4	-	P_{ij} $-\kappa\gamma_{ij}$	no	no	makes 2 Neg.	not apparent	makes 2 Neg.	not apparent
P-5	-	P_{ij} $-\kappa\gamma_{rr}$	no	no	red. Pos./enl.Neg.	not apparent	red.Pos./enl.Neg.	not apparent
Q-1	-	$Q^k{}_{ij}$ $\kappa\alpha\beta^k\gamma_{ij}$	no	no	N/A	N/A	$\kappa\sim 1.35$ min. vals.	not apparent
Q-2	-	$Q^k{}_{ij}$ $Q^r{}_{rr}=\kappa$	no	yes	red. abs vals.	not apparent	red. abs vals.	not apparent
Q-3	-	$Q^k{}_{ij}$ $Q^r{}_{ij}=\kappa\gamma_{ij}$ or $Q^r{}_{ij}=\kappa\alpha\gamma_{ij}$	no	yes	red. abs vals.	not apparent	enl.Neg.	enl. vals.
Q-4	-	$Q^k{}_{ij}$ $Q^r{}_{rr}=\kappa\gamma_{rr}$	no	yes	red. abs vals.	not apparent	red. abs vals.	not apparent
R-1	1	R_{ij} $\kappa_F\alpha\gamma_{ij}$	yes	yes	$\kappa_F=-1/4$ min. abs vals.		$\kappa_F=-1/4$ min. vals.	
R-2	4	R_{ij} $R_{rr}=-\kappa_\mu\alpha$ or $R_{rr}=-\kappa_\mu$	yes	no	not apparent	not apparent	red.Pos./enl.Neg.	enl. vals.
R-3	-	R_{ij} $R_{rr}=-\kappa\gamma_{rr}$	yes	no	enl. vals.	not apparent	red.Pos./enl.Neg.	enl. vals.
S-1	2-S	$S^k{}_{ij}$ $\kappa_L\alpha^2[3(\partial_{(i}\alpha)\delta^k_{j)}-(\partial_l\alpha)\gamma_{ij}\gamma^{kl}]$	yes	no	not apparent	not apparent	not apparent	not apparent
S-2	-	$S^k{}_{ij}$ $\kappa\alpha\gamma^{lk}(\partial_l\gamma_{ij})$	yes	no	makes 2 Neg.	not apparent	makes 2 Neg.	not apparent
p-1	-	$p^k{}_{ij}$ $p^r{}_{ij}=-\kappa\alpha\gamma_{ij}$	no	no	red. Pos.	red. vals.	red. Pos.	enl. vals.
p-2	-	$p^k{}_{ij}$ $p^r{}_{rr}=\kappa\alpha$	no	no	red. Pos.	red. vals.	red.Pos/enl.Neg.	enl. vals.
p-3	-	$p^k{}_{ij}$ $p^r{}_{rr}=\kappa\alpha\gamma_{rr}$	no	no	makes 2 Neg.	enl. vals.	red. Pos. vals.	red. vals.
q-1	-	$q^{kl}{}_{ij}$ $q^{rr}{}_{ij}=\kappa\alpha\gamma_{ij}$	no	no	$\kappa=1/2$ min. vals.	red. vals.	not apparent	enl. vals.
q-2	-	$q^{kl}{}_{ij}$ $q^{rr}{}_{rr}=-\kappa\alpha\gamma_{rr}$	no	yes	red. abs vals.	not apparent	not apparent	not apparent
r-1	-	$r^k{}_{ij}$ $r^r{}_{ij}=\kappa\alpha\gamma_{ij}$	no	yes	not apparent	not apparent	not apparent	enl. vals.
r-2	-	$r^k{}_{ij}$ $r^r{}_{rr}=-\kappa\alpha$	no	yes	red. abs vals.	enl. vals.	red. abs vals.	enl. vals.
r-3	-	$r^k{}_{ij}$ $r^r{}_{rr}=-\kappa\alpha\gamma_{rr}$	no	yes	red. abs vals.	enl. vals.	red. abs vals.	enl. vals.
s-1	2-s	$s^{kl}{}_{ij}$ $\kappa_L\alpha^3[\delta^k_{(i}\delta^l_{j)}-(1/3)\gamma_{ij}\gamma^{kl}]$	no	no	makes 4 Neg.	not apparent	makes 4 Neg.	not apparent
s-2	-	$s^{kl}{}_{ij}$ $s^{rr}{}_{ij}=-\kappa\alpha\gamma_{ij}$	no	no	makes 2 Neg.	red. vals.	makes 2 Neg.	red. vals.
s-3	-	$s^{kl}{}_{ij}$ $s^{rr}{}_{rr}=-\kappa\alpha\gamma_{rr}$	no	no	makes 2 Neg.	red. vals.	makes 2 Neg.	red. vals.

TABLE III: List of adjustments we tested in the Schwarzschild spacetime. The column of adjustments are nonzero multipliers in terms of (2.13) and (2.14). The column '1st?' and 'TRS' are the same as Table. I. The effects to amplification factors (when $\kappa>0$) are commented for each coordinate system and for real/imaginary parts of AFs, respectively. The 'N/A' means that there is no effect due to the coordinate properties; 'not apparent' means the adjustment does not change the AFs effectively according to our conjecture; 'enl./red./min.' means enlarge/reduce/minimize, and 'Pos./Neg.' means positive/negative, respectively. These judgements are made at the $r\sim O(10M)$ region on their $t=0$ slice.

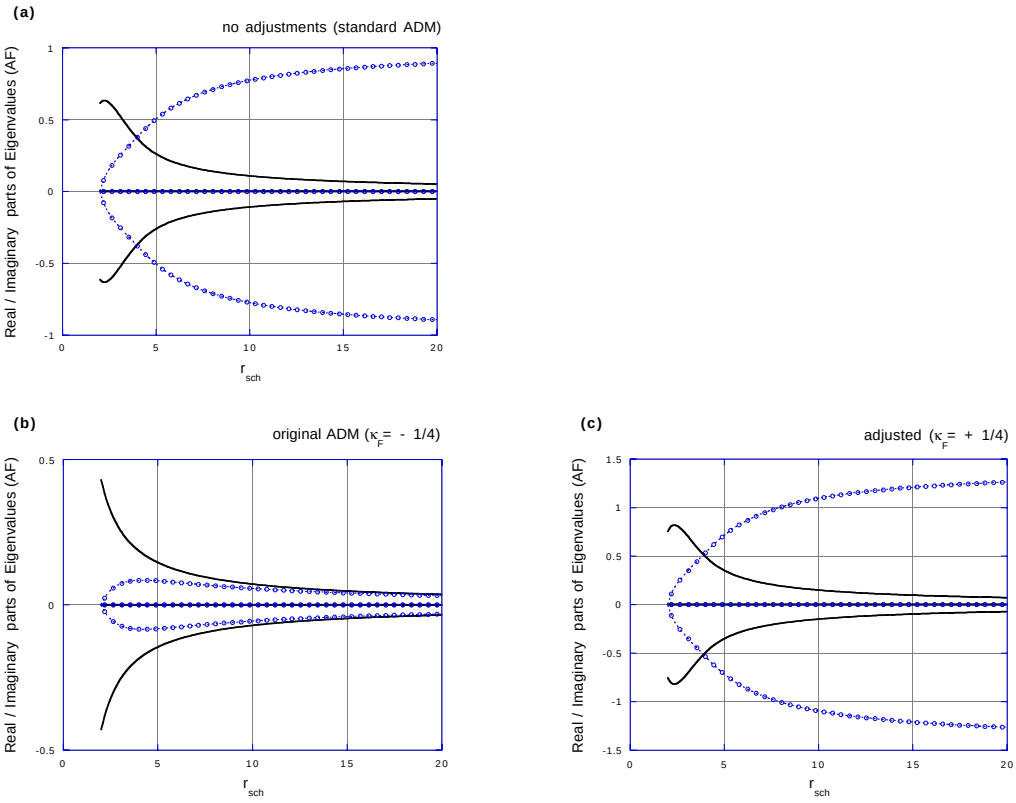

FIG. 1: Amplification factors (AFs, eigenvalues of homogenized constraint propagation equations) are shown for the standard Schwarzschild coordinate, with (a) no adjustments, i.e., standard ADM, (b) original ADM ($\kappa_F = -1/4$) and (c) an adjusted version with different signature, $\kappa_F = +1/4$ [see eq. (2.17)]. The solid lines and the dotted lines with circles are real parts and imaginary parts, respectively. They are four lines each, but actually the two eigenvalues are zero for all cases. Plotting range is $2 < r \leq 20$ using Schwarzschild radial coordinate. We set $k = 1, l = 2$, and $m = 2$ throughout the article.

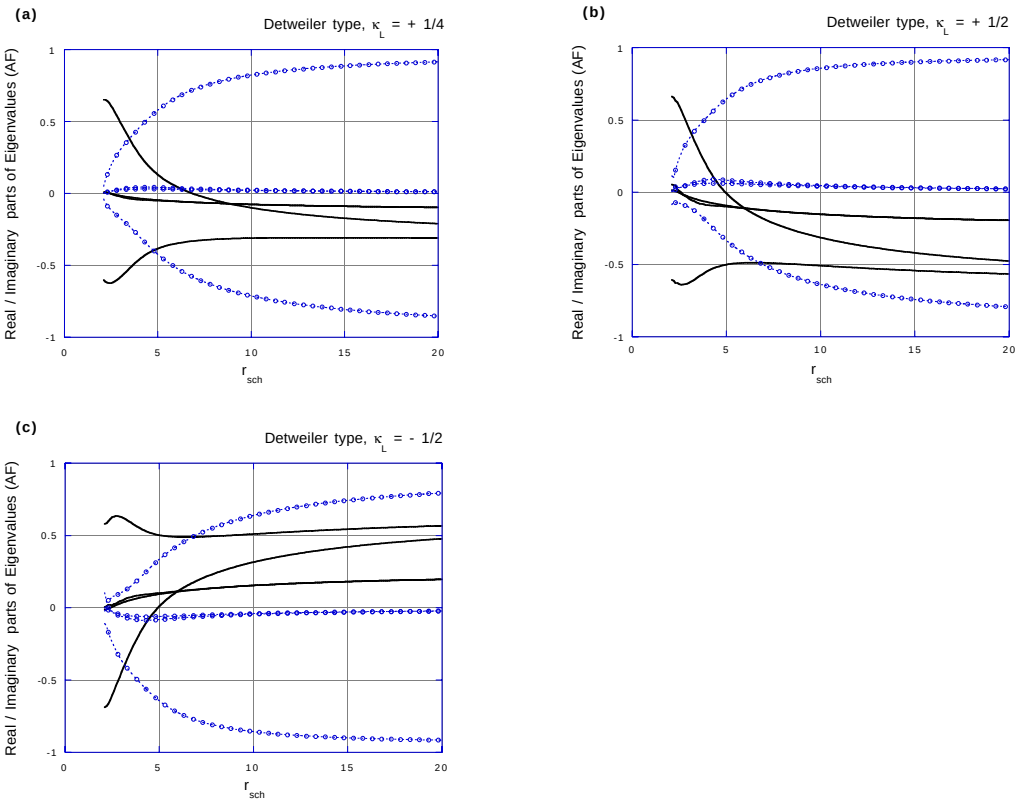

FIG. 2: Amplification factors of the standard Schwarzschild coordinate, with Detweiler type adjustments, (2.18)-(2.21). Multipliers used in the plot are (a) $\kappa_L = +1/4$, (b) $\kappa_L = +1/2$, and (c) $\kappa_L = -1/2$. Plotting details are the same as Fig.1.

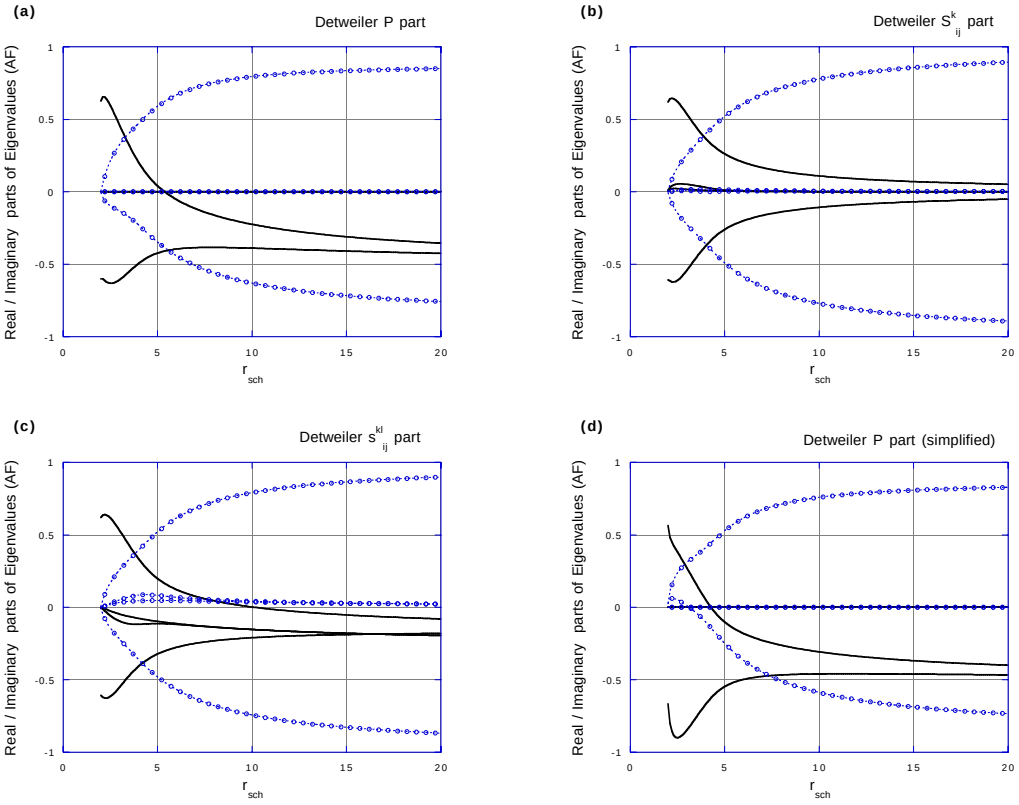

FIG. 3: Amplification factors of the standard Schwarzschild coordinate, with Detweiler type (partial contributions) adjustments. Fig.(a) is the case No. 2-P in Table.I, adjusting with $P_{ij} = -\kappa_L \alpha^3 \gamma_{ij}$, i.e. (2.18), and else zero. Similarly, (b) is No. 2-S, ${S^k}_{ij}$-part (2.20) and else zero, and (c) is No. 2-s, ${s^{kl}}_{ij}$-part (2.21) and else zero. Fig. (d) is No. 3, $P_{ij} = -\kappa_L \alpha \gamma_{ij}$ and else zero, which is a minor modification from (a). We used $\kappa_L = +1/2$ for all plots. Plotting details are the same as Fig.1.

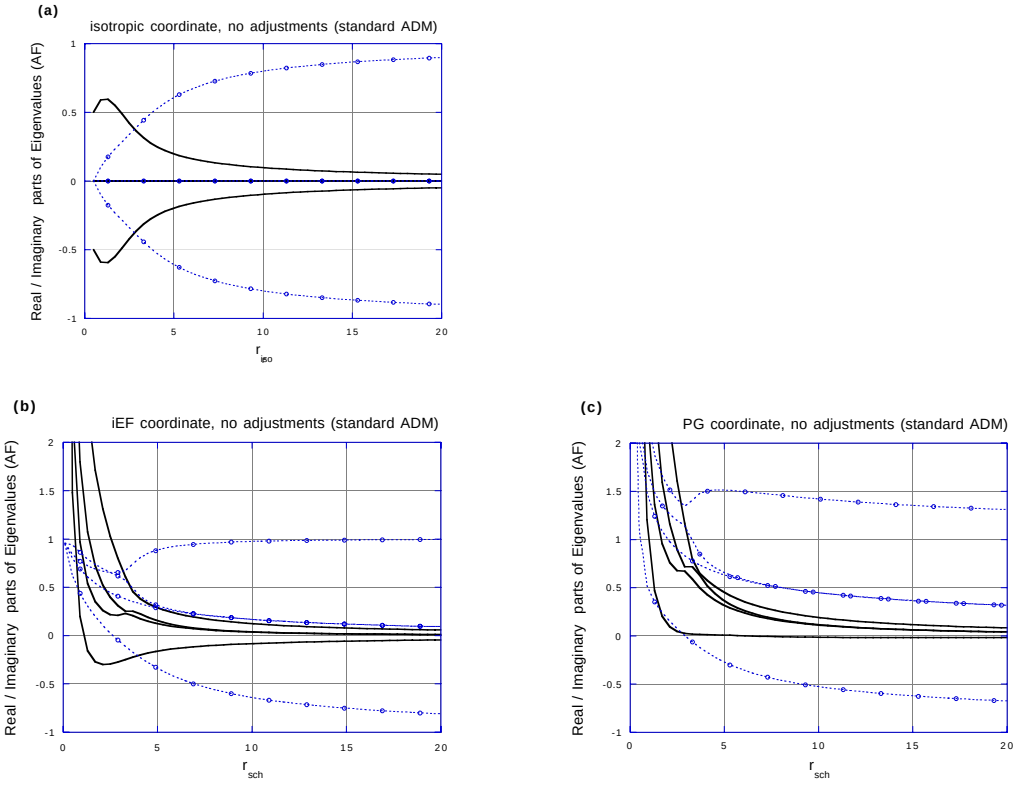

FIG. 4: Comparison of amplification factors between different coordinate expressions for the standard ADM formulation (i.e. no adjustments). Fig. (a) is for the isotropic coordinate (4.2), and the plotting range is $1/2 \leq r_{iso}$. Fig. (b) and (c) are for the iEF coordinate (4.3) and the PG coordinate (4.4), respectively, and we plot lines on the $t = 0$ slice for each expression. [See Fig.1(a) for the standard Schwarzschild coordinate.] The solid four lines and the dotted four lines with circles are real parts and imaginary parts, respectively.

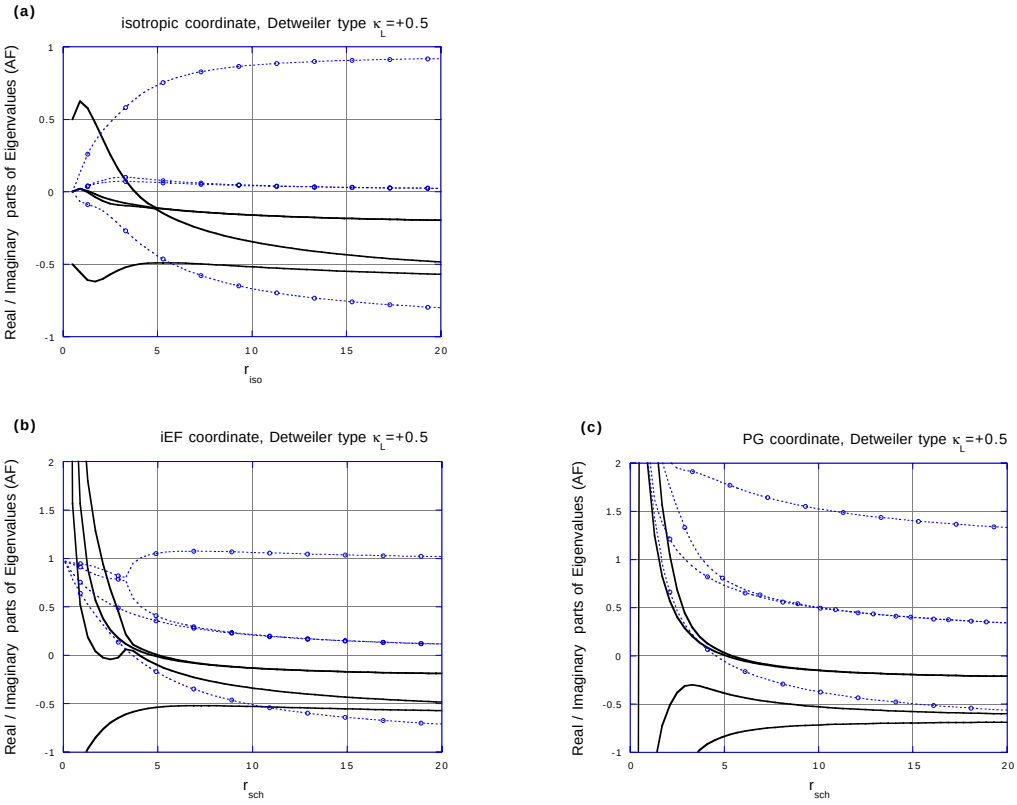

FIG. 5: Similar comparison with Fig.4, but for Detweiler adjustments. $\kappa_L = +1/2$ for all plots. [See Fig.2(b) for the standard Schwarzschild coordinate.]

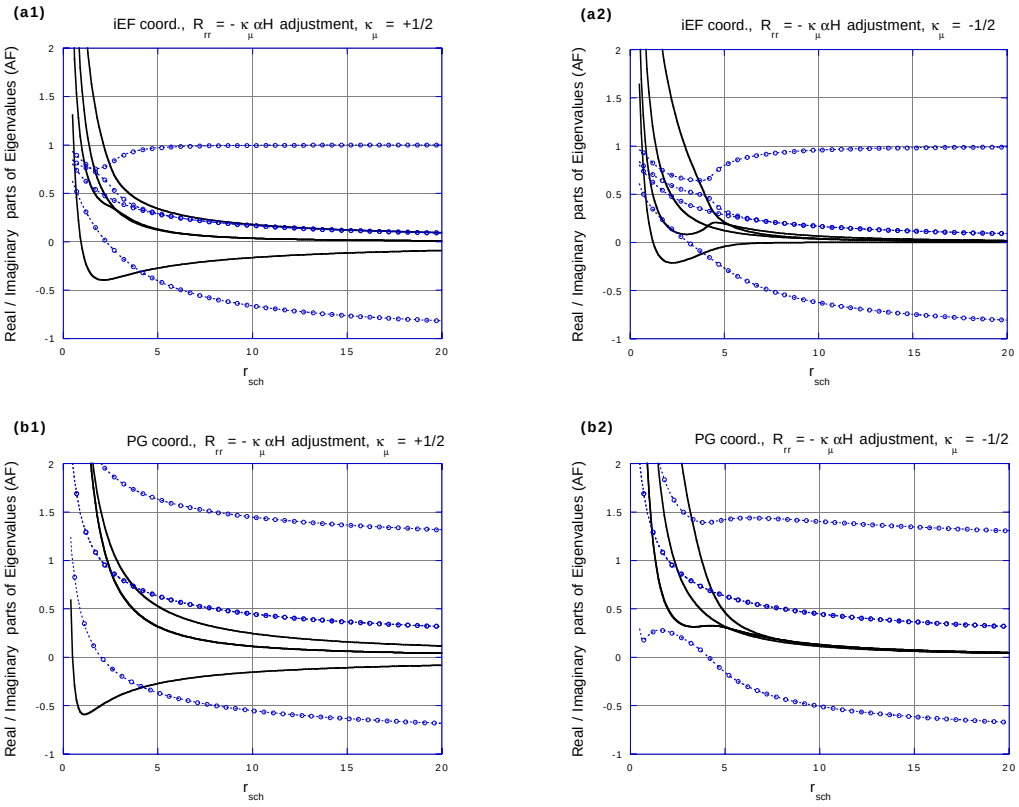

FIG. 6: Amplification factors of the adjustment No.4 in Table. I. $\kappa_\mu = +1/2, -1/2$ for iEF/PG coordinates. [See Fig.4(b)(c) for the standard ADM system.]

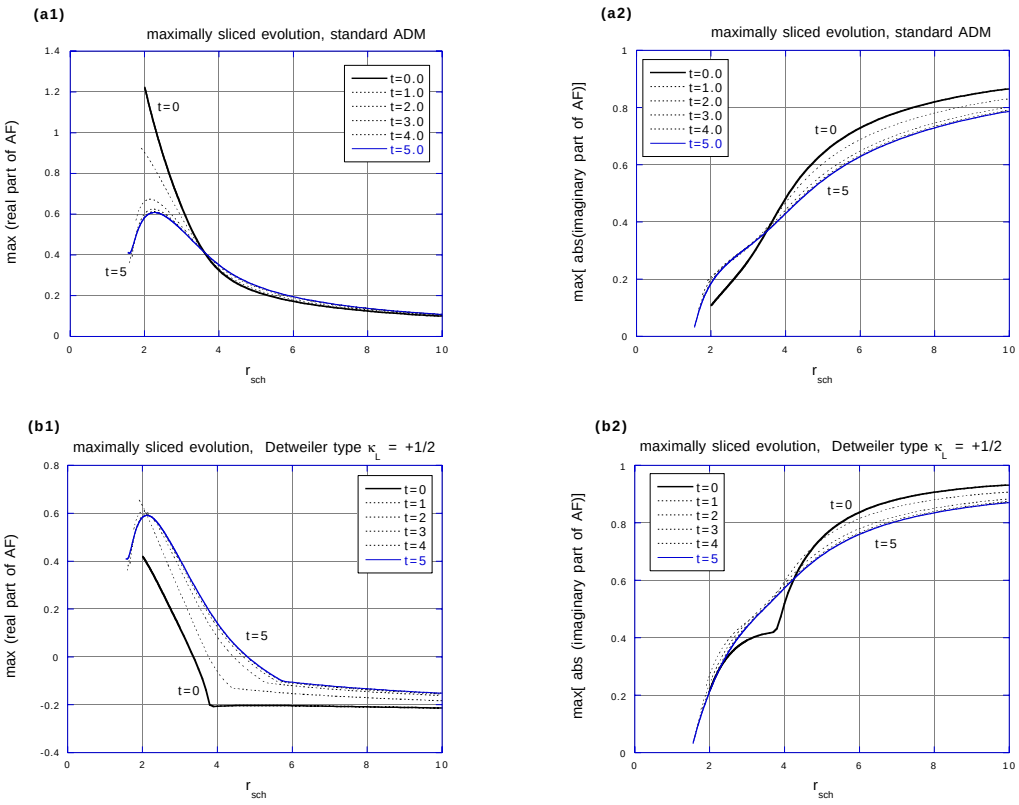

FIG. 7: Amplification factors of snapshots of maximally-sliced evolving Schwarzschild spacetime. Fig (a1) and (a2) are of the standard ADM formulation (real and imaginary parts, respectively), (b1) and (b2) are Detweiler's adjustment ($\kappa_L = +1/2$). Lines in (a1) and (b1) are the largest (positive) AF on each time slice, while lines in (a2) and (b2) are the maximum imaginary part of AF on each time slice. The time label t in plots is $\bar{t}$ in Appendix B. The lines start at $r_{min} = 2$ ($\bar{t} = 0$) and $r_{min} = 1.55$ ($\bar{t} = 5$).